

SUPPORTING INFORMATION

[NH₂CHNH₂]₃Sb₂I₉: Lead-Free and Low-Toxicity Organic-Inorganic Hybrid Ferroelectric Based on Antimony(III) as a Potential Semiconducting Absorber

Przemysław Szklarz[†], Ryszard Jakubas[†], Anna Gągor^{††}, Grażyna Batort[†], Jakub Cichos[†] and Mirosław Karbowski[†]

[†]Faculty of Chemistry, University of Wrocław, F. Joliot-Curie 14, 50-383 Wrocław, Poland

^{††}W. Trzebiatowski Institute of Low Temperature and Structure Research PAS, P.O. Box 1410, 50-950 Wrocław, Poland.

The ferroelectric hysteresis loop measurements were carried out for several temperatures between 140 K and room temperature. This range covers all solid state phases found for FAIA during the DSC studies. The measurements were carried out using the Radiant Precision Premier II Ferroelectric Tester. In the experiments, alternating voltage with a triangular waveform of a frequency between 0.1 and 100 Hz was applied. The value of the applied voltage amplitude was 500 V (for samples with a thickness of $d \sim 1$ mm)."

Table S1. Crystal data, data collection and refinement of **FAIA** in phase I

Crystal data	
Chemical formula	C ₃ H ₁₅ I ₉ N ₆ Sb ₂
M_r	1520.81
Crystal system, space group	Hexagonal, $P6_3mc$
Temperature (K)	195
a, c (Å)	8.699(1), 21.678 (1)
V (Å ³)	1420.8(1)
Z	2
Radiation type	Mo $K\alpha$
μ (mm ⁻¹)	11.68
Crystal size (mm)	0.21 × 0.17 × 0.08
Data collection	
Diffractionmeter	Xcalibur, Atlas
Absorption correction	Multi-scan,
T_{\min}, T_{\max}	0.362, 1.000
No. of measured, independent and observed [$I > 2\sigma(I)$] reflections	10329, 1097, 897
R_{int}	0.038
$(\sin \theta/\theta)_{\text{max}}$ (Å ⁻¹)	0.610
Refinement	
$R[F^2 > 2\sigma(F^2)], wR(F^2), S$	0.053, 0.123, 1.65
No. of reflections	1097
No. of parameters	43
No. of restraints	8
H-atom treatment	H-atom parameters constrained
$\Delta\rho_{\text{max}}, \Delta\rho_{\text{min}}$ (e Å ⁻³)	0.84, -0.95
Absolute structure	Refined as an inversion twin.

Table S2. Selected geometric parameters in phase I (Å, °)

Sb1—I1 ⁱ	2.881 (6)	Sb2—I3 ⁱⁱ	2.859 (5)
Sb1—I1 ⁱⁱ	2.881 (6)	Sb2—I3 ⁱ	2.859 (5)
Sb1—I1	2.881 (6)	Sb2—I3	2.859 (5)
Sb1—I2 ⁱ	3.213 (5)	Sb2—I2	3.224 (5)
Sb1—I2 ⁱⁱ	3.213 (5)	Sb2—I2 ⁱⁱ	3.224 (5)
Sb1—I2	3.213 (5)	Sb2—I2 ⁱ	3.224 (5)
I—Sb1—I _{cis}	83.9 (2) - 92.6 (2)	I—Sb2—I _{cis}	83.5 (2) - 94.4 (2)
I—Sb1—I _{trans}	173.9(2)	I—Sb2—I _{trans}	172.4 (2)

Symmetry code(s): (i) $-y+1, x-y+1, z$; (ii) $-x+y, -x+1, z$.

Table S3. Selected hydrogen-bond parameters

D—H...A	D—H (Å)	H...A (Å)	D...A (Å)	D—H...A (°)
N2—H2A...I3 ⁱ	0.86	2.88	3.69 (9)	157.2
N3—H3B...I1 ⁱⁱ	0.86	3.04	3.83 (7)	152.3
N7—H7B...I1	0.86	2.48	3.255 (7)	150.8
N7—H7A...I3 ⁱⁱⁱ	0.86	2.68	3.41 (3)	144.0
N5—H5B...I2 ^{iv}	0.86	2.90	3.60 (5)	139.5

Symmetry code(s): (i) $-x+y, -x, z$; (ii) $x-1, y-1, z$; (iii) $-x+1, -y+1, z-1/2$; (iv) $-y+1, x-y, z$.

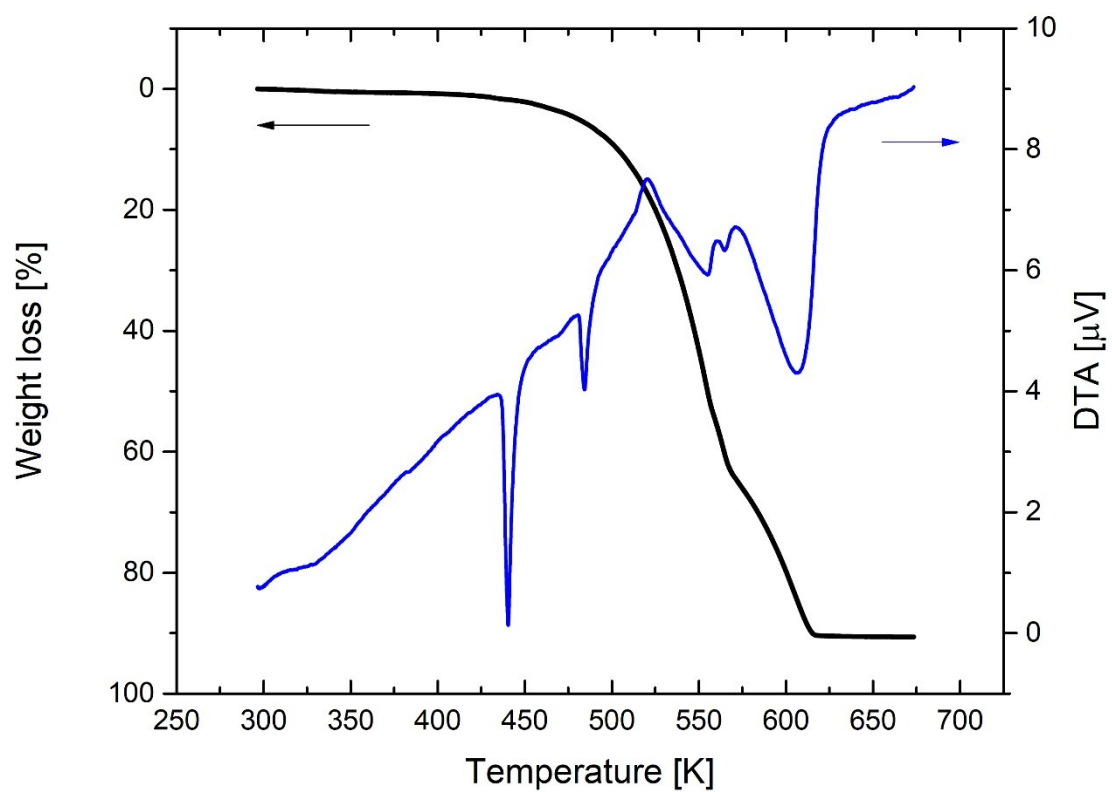


Fig S1. The TGA and DTA signals for **FAIA**.

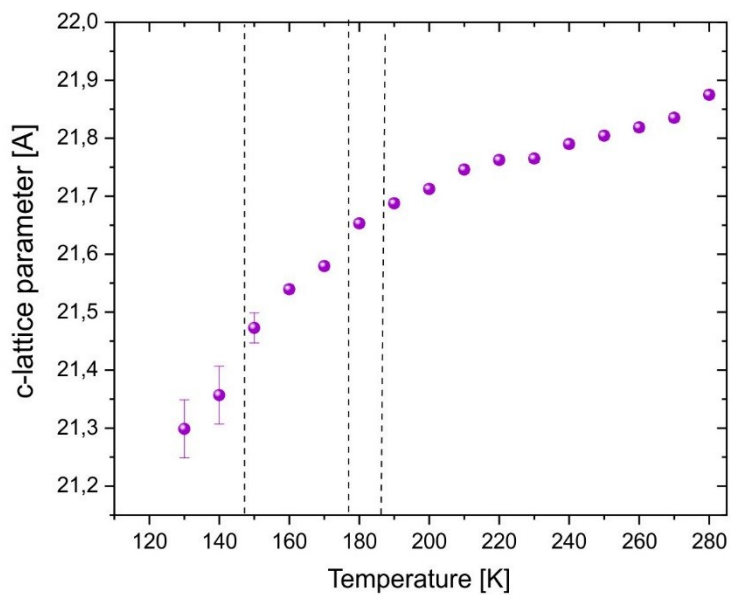


Fig S2. The thermal evolution of the c-lattice parameter for **FAIA**.

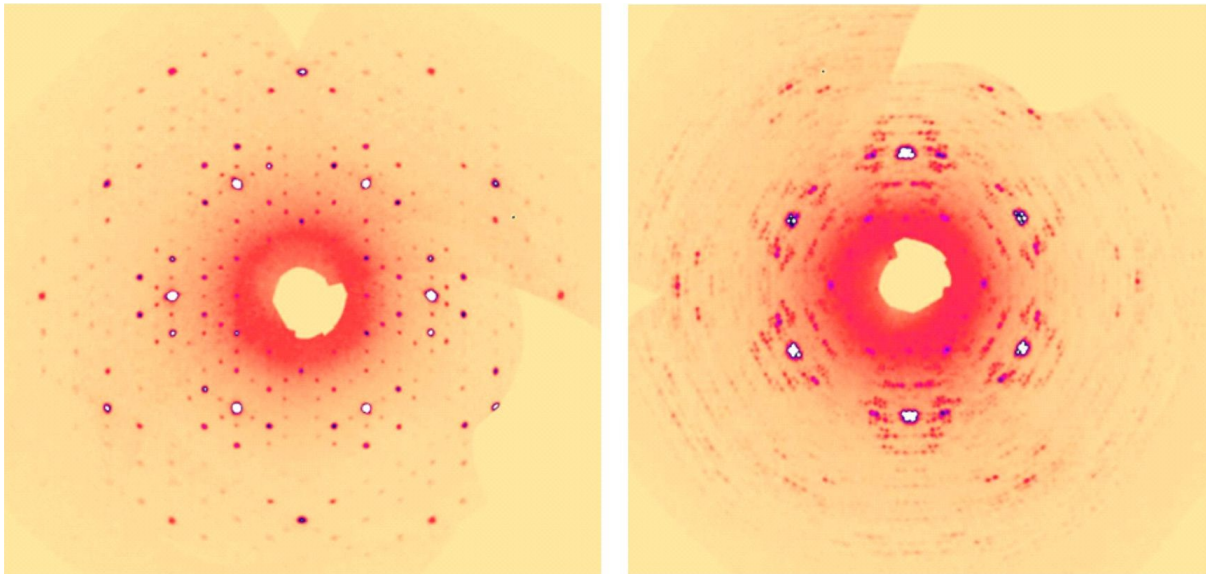


Fig. S3. Reconstructions of the reciprocal lattice ($hk0$ layer) in phase III, $T=168\text{K}$, showing pseudo-hexagonal lattice with weak satellites (on the left) and Phase IV, $T=100\text{K}$ with distinct splitting of diffracted intensities (on the right).

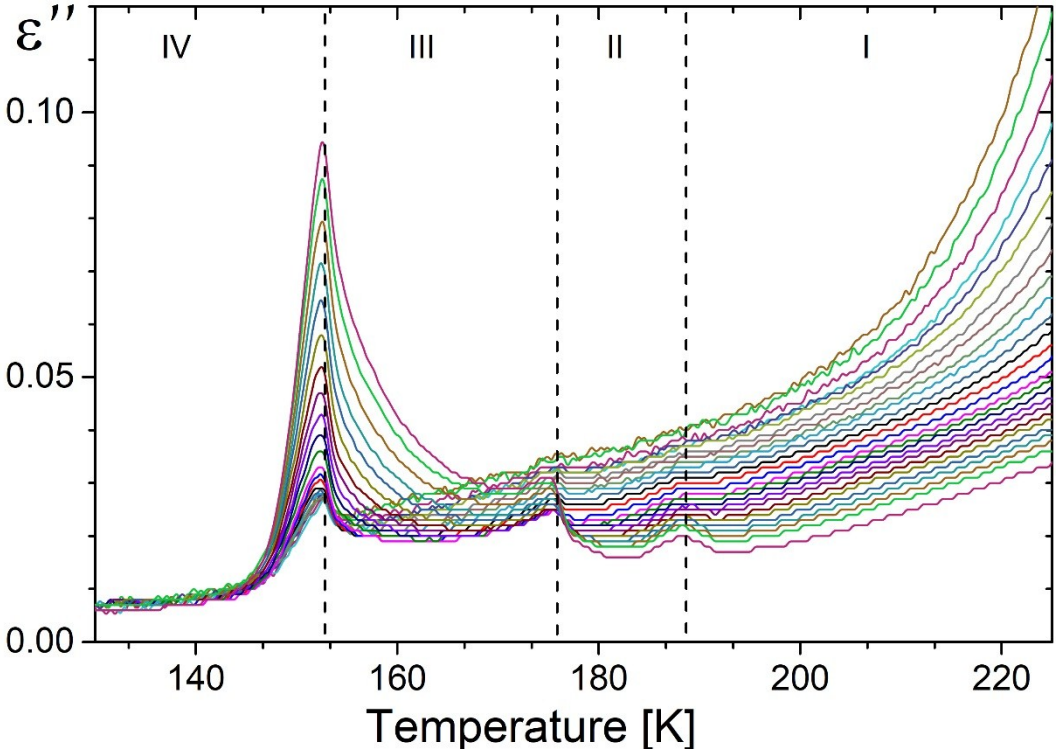


Fig. S4. The temperature dependence of the imaginary part of the complex electric permittivity of **FAIA**.

The conductivity from the alternating current measurements is a complex quantity given by the formula:

$$\sigma_{ac}(T,\omega) = \sigma_{dc}(T) + \varepsilon_0\omega\varepsilon''(T,\omega) + i\varepsilon_0\omega\varepsilon'(T,\omega), \quad (1)$$

where σ_{dc} corresponds to the direct current conductivity, which is a material property and should be frequency-independent, the second part is the real part of the conductivity and the latter comes

from the imaginary contribution of σ_{ac}^* .

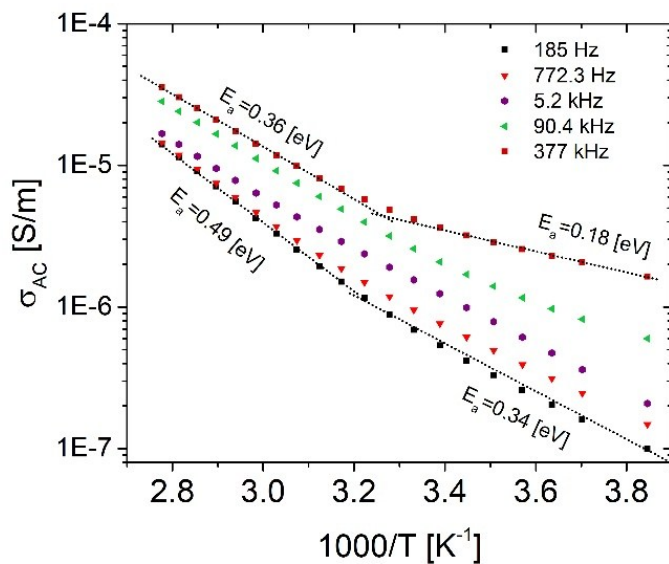


Fig. S5. The dependence of the *ac* conductivity [$S\ m^{-1}$] (*log* scale) versus reciprocal temperature, $1000/T$, from alternating current measurements for **FAIA**.

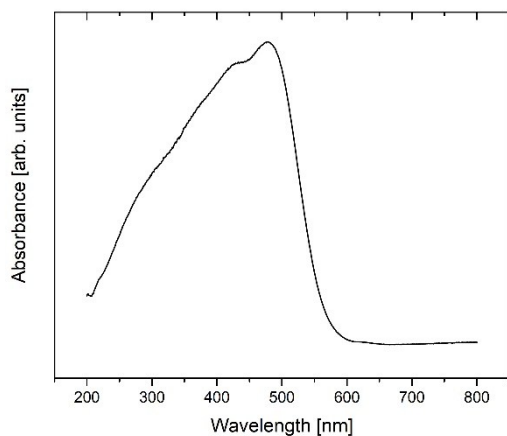


Fig. S6. Absorption spectrum for **FAIA**.

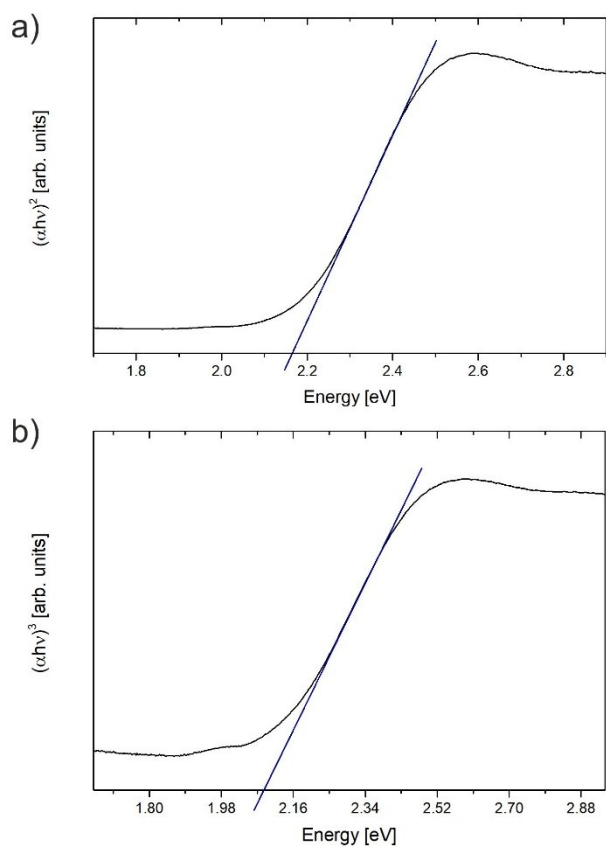


Fig. S7. Tauc plot of **FAIA** for $r=2$ (a) and $r=3$ (b).

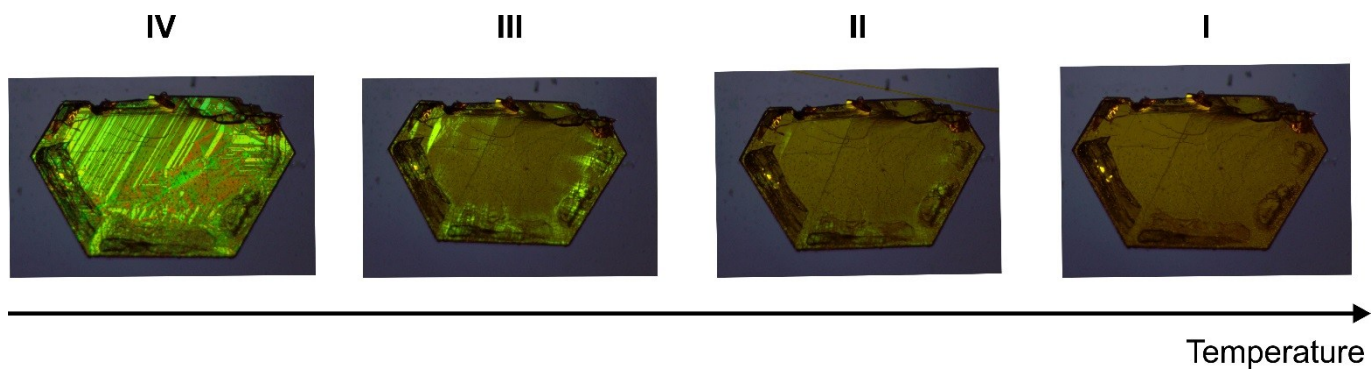


Fig. S8. The evolution of the ferroelastic domain pattern for **FAIA** during the cooling cycle